



Mitochondrial dysfunction-related lipid changes occur in nonalcoholic fatty liver disease progression^S

Kang-Yu Peng,^{*,†} Matthew J. Watt,[§] Sander Rensen,^{**} Jan Willem Greve,^{††} Kevin Huynh,^{*} Kaushala S. Jayawardana,^{*} Peter J. Meikle,^{1,2,*,†} and Ruth C. R. Meex^{1,2,§§}

Baker Heart and Diabetes Institute,^{*} Melbourne, Victoria, Australia; Department of Biochemistry and Molecular Biology,[†] University of Melbourne, Parkville, Victoria, Australia; Department of Physiology,[§] Faculty of Medicine, Dentistry, and Health Sciences, University of Melbourne, Melbourne, Victoria, Australia; Departments of Surgery^{**} and Human Biology,^{§§} NUTRIM School of Nutrition and Translational Research in Metabolism, Maastricht University Medical Centre, Maastricht, The Netherlands; and Department of Surgery,^{††} Zuyderland Medical Center Heerlen, Heerlen, The Netherlands

Abstract Nonalcoholic fatty liver disease (NAFLD) comprises fat-accumulating conditions within hepatocytes that can cause severe liver damage and metabolic comorbidities. Studies suggest that mitochondrial dysfunction contributes to its development and progression and that the hepatic lipiome changes extensively in obesity and in NAFLD. To gain insight into the relationship between lipid metabolism and disease progression through different stages of NAFLD, we performed lipidomic analysis of plasma and liver biopsy samples from obese patients with nonalcoholic fatty liver (NAFL) or nonalcoholic steatohepatitis (NASH) and from those without NAFLD. Congruent with earlier studies, hepatic lipid levels overall increased with NAFLD. Lipid species that differed with NAFLD severity were related to mitochondrial dysfunction; specifically, hepatic cardiolipin and ubiquinone accumulated in NAFL, and levels of acylcarnitine increased with NASH. We propose that increased levels of cardiolipin and ubiquinone may help to preserve mitochondrial function in early NAFLD, but that mitochondrial function eventually fails with progression to NASH, leading to increased acylcarnitine. We also found a negative association between hepatic odd-chain phosphatidylcholine and NAFLD, which may result from mitochondrial dysfunction-related impairment of branched-chain amino acid catabolism. Overall, these data suggest a close link between accumulation of specific hepatic lipid species, mitochondrial dysfunction, and the progression of NAFLD.—Peng, K.-Y., M. J. Watt, S. Rensen, J. W. Greve, K. Huynh, K. S. Jayawardana, P. J. Meikle, and R. C. R. Meex. Mitochondrial dysfunction-related lipid changes occur in nonalcoholic fatty liver disease progression. *J. Lipid Res.* 2018. 59: 1977–1986.

Supplementary key words lipidomics • liver metabolism • mitochondria • obesity

This work was supported by National Health and Medical Research Council Grant APP1061278. Additional support was provided by an International Scholarship from the University of Melbourne (K.-Y.P.); National Health and Medical Research Council Senior Research Fellowships APP1077703 and APP1042095 (M.J.W., P.J.M.); and H2020 Marie Skłodowska-Curie Actions Grant H2020-MSCA-IF (R.C.R.M.).

Manuscript received 3 April 2018 and in revised form 19 July 2018.

Published, *JLR Papers in Press*, July 24, 2018
DOI <https://doi.org/10.1194/jlr.M085613>

Copyright © 2018 Peng et al. Published under exclusive license by The American Society for Biochemistry and Molecular Biology, Inc.

This article is available online at <http://www.jlr.org>

Nonalcoholic fatty liver disease (NAFLD) is an umbrella term that is used to describe a variety of conditions characterized by a build-up of fat within liver cells. NAFLD can range from mild hepatic steatosis [nonalcoholic fatty liver (NAFL)] to the more severe nonalcoholic steatohepatitis (NASH), and can progress to fibrosis, cirrhosis, and hepatocellular carcinoma. NAFLD is the predominant cause of chronic liver disease in many parts of the world, and is present in 75–90% of adults who are morbidly obese (1, 2). Given that the liver is a central regulator of whole-body energy homeostasis, it is not surprising that many individuals with NAFLD are also characterized by metabolic complications, including insulin resistance, muscle atrophy, and cardiovascular disease, resulting in increased morbidity and mortality (3).

NAFL is diagnosed when liver fat exceeds 5% of the total liver weight. Lipid accumulation in the liver is regulated by the interplay between the delivery of lipids to the liver and their hepatic uptake, synthesis, oxidation, and secretion of lipids. Alterations in the equilibrium of one or more of these processes can promote hepatic steatosis (4). NASH is characterized by hepatic steatosis, hepatocyte ballooning, and lobular inflammation. The mechanisms that trigger hepatic inflammation are poorly understood, and to date, a liver biopsy is the only reliable method to distinguish between the different stages of NAFLD. Several studies have tried to identify lipid biomarkers of NAFL and NASH, but

Abbreviations: BCAA, branched-chain amino acid; CE, cholesteryl ester; CTRL, control; DG, diacylglycerol; DUFA, diunsaturated FA; HOMA-IR, homeostatic model assessment of insulin resistance; NAFL, nonalcoholic fatty liver; NAFLD, nonalcoholic fatty liver disease; NASH, nonalcoholic steatohepatitis; PC, phosphatidylcholine; SFA, saturated FA; TG, triacylglycerol.

¹P. J. Meikle and R. C. R. Meex are co-senior authors.

²To whom correspondence should be addressed.

e-mail: ruth.meex@maastrichtuniversity.nl (R.C.R.M.);

peter.meikle@baker.edu.au (P.J.M.)

^SThe online version of this article (available at <http://www.jlr.org>) contains a supplement.

this has proven to be very difficult because the correlations between blood and liver lipid species drastically decrease after the transition from NAFL to NASH (5). We previously used lipidomics to compare serum lipid profiles from excessive chronic drinkers without liver disease to those with advanced alcoholic cirrhosis, and showed that circulating lipids associate with alcoholic liver cirrhosis and represent potential biomarkers for risk assessment (6). The aim of the current study was to gain a more comprehensive understanding of the hepatic and plasma lipidomic changes in morbidly obese subjects with NAFL or NASH compared with morbidly obese subjects without NAFLD, and to gain insight into lipid species that are linked to disease progression through the different stages of NAFLD. We performed lipidomic analysis in liver biopsies and plasma samples from 58 subjects classified on the basis of liver histology as either normal ($n = 16$), steatotic ($n = 10$), or NASH ($n = 32$).

MATERIALS AND METHODS

Study cohort

Our study cohort consisted of 58 subjects with severe obesity (BMI >35) who underwent bariatric surgery. The institutional medical ethical committee of Maastricht University approved the study, and all subjects gave written informed consent before participation in the study. Just before surgery, a fasting venous blood sample was obtained from each subject. During surgery, a fasted liver biopsy was obtained. Part of the liver biopsies were fixed in formalin and embedded in paraffin, and histopathology was performed by H&E staining and Masson's trichrome staining. Subjects were classified as control (CTRL), NAFL, or NASH according to the criteria of both Brunt et al. (7) and Kleiner et al. (8). The CTRL group was comprised of subjects showing <5% steatotic hepatocytes. The steatotic group was comprised of individuals showing >5% steatotic hepatocytes without significant inflammation, as observed after H&E staining (no intra-acinar inflammatory foci per 20 fields with a 20 ocular and no portal tract inflammation). The third group was comprised of subjects with NASH, who were identified by the presence of steatosis, lobular inflammation, and hepatocellular ballooning.

Sample preparation and lipid extraction

Lipid extraction of the liver and plasma was carried out using an earlier described single-phase chloroform:methanol (2:1) approach, with some modifications (9). Briefly, liver tissues (weighing ~0.7–1.9 mg) were first homogenized with a Bullet Blender[®] Gold homogenizer (Next Advance, Inc., Averill Park, NY) in 250 μ l Tris-NaCl containing 100 μ M of butylhydroxytoluene, and then underwent further probe sonication (S-4000, Misonix Ultrasonic, amplitude 26, 30 s on ice; Misonix) to break down the tissue completely. For lipid extraction, a 10 μ l liver or plasma sample was mixed with 200 μ l of chloroform/methanol (2:1 v/v) and 10 μ l of internal standard mix (supplemental Table S1). The samples were rotary mixed and sonicated for 30 min at room temperature, then centrifuged (16,000 g, 15 min) to remove the insoluble pellets. The supernatants were then transferred to 96-well plates and dried using the Speedy Vac system (Savant RVT5105; Thermo Fisher Scientific). Prior to lipidomic analysis, the lipid extract was dried and redissolved in 50 μ l of water-saturated butanol. Then, 50 μ l of methanol containing 10 mM ammonium formate were added. The samples were subsequently centrifuged (3,350 g, 5 min, room temperature), and the supernatant containing the

reconstituted lipids was transferred to glass vials (with glass inserts) for LC-MS lipidomic analysis.

Lipid profiling

Targeted lipidomics for the liver and plasma specimens was performed using LC coupled with an electrospray ionization Qtrap 4000 mass spectrometer (AB Sciex), as described earlier with slight modifications (10). HPLC separation was conducted using an Agilent 1200 series HPLC system with a Poroshell 120 EC-C18 column (2.1 \times 100 mm, 2.7 microns; Agilent) with the thermostat set at 50°C. The solvent system consisted of solvent A [60% water, 20% methanol, and 20% THF (v/v/v) with 10 mM ammonium formate] and solvent B [75% THF, 20% methanol, and 5% water (v/v/v) with 10 mM ammonium formate]. Our gradient was as follows: starting conditions at 90% A 10% B, increasing to 20% B over 0.1 min then increasing to 35% B at 3 min, 50% B at 3.5 min, 62% B at 11 min, followed by a sharp adjustment to 89% B at 11.1 min with a shallow gradient to 92% B at 14.9 min then adjusting to 100% B at 15 min and holding until 16.5 min. The gradient was then adjusted back to starting conditions at 17 min and held for 3 min for a final run time of 20 min. This method enabled all lipid species, including diacylglycerol (DG) and triacylglycerol (TG) species, to be monitored in a single chromatographic run. As in the previous method, the quantification of the TG species was based on the neutral loss of a FA (+NH₄) and the remaining FAs were assigned based on comprehensive neutral loss scans of each FA type using the pooled plasma quality control sample. Thus, we were able to differentiate the TG species containing 17:0 acyl chains (e.g., TG(16:0_17:0_18:1) from the internal standard [TG(17:0/17:0/17:0)] based on precursor mass (m/z 864.8 and m/z 866.8), the neutral loss [299.3 Da (18:1) and 287.2 Da (17:0)], and the retention time (15.65 min and 15.94 min). A total of 474 lipid species across 29 lipid classes and subclasses were detected in this study (supplemental Table S1). AB Sciex MultiQuant software version 2.1.1 (AB Sciex) was used for quantification of peaks and data integration.

Phospholipid isomer characterization

Under normal analysis conditions, we were unable to obtain phospholipid acyl composition. However, our current chromatography allowed separation of isomers by their retention time. To facilitate identification, the FA composition of phospholipids was characterized by either collision-induced dissociation in negative ionization mode, for neutral or negatively charged species, or by collision-induced dissociation of lithium adducts in positive ionization mode for positively charged species, and subsequently used to infer structural composition of phospholipid isomers based on retention time for species that were well separated. Characterization of the phospholipid FAs was performed on whole lipid extracts of pooled plasma samples. For the analysis of lithium adducts of phosphatidylcholine (PC), alkylphosphatidylcholine, alkenylphosphatidylcholine, and SM, the 10 mM of ammonium formate in the extraction buffer and running solvents were substituted with 200 μ M of lithium acetate, which provided the ability to monitor for lithium adducts for additional structural information (11, 12). Where it was not possible to definitively characterize isomers (typically resulting from double bond position), we adopted the system of annotating with an (a) and a (b).

Statistical analysis

Patient characteristics are presented as mean \pm SEM (numerical data) or percent (categorical data). For 15 out of 18 characteristics shown, there was at least one missing data point (maximum seven missing for any characteristics), and they were estimated with the imputation approach. The missing data were imputed using the multiple imputation by chained equations (MICE)

method, utilizing the R package “mice”. The numerical data were analyzed with the Mann-Whitney U test, while the categorical data were analyzed with the χ^2 test. A *P* value <0.05 was considered significant. The liver and plasma lipidomic data are presented as picomoles per micromole of PC. Mean \pm SEM or percent difference to the CTRL group are used to display the lipidomic data. The Kruskal-Wallis test corrected with the Benjamini-Hochberg approach was used to determine the inter-group significance. A corrected *P* value <0.05 was considered significant. Mann-Whitney U tests corrected with the Dunn-Sidak approach were utilized as the post hoc test, and a *P* value <0.05 was considered significant. To determine the association of the lipid species or classes to the disease (i.e., NAFL and NASH), logistic regression was performed between CTRL, NAFL, and NASH. The Benjamini-Hochberg approach was applied for multiple comparisons, and a *P* value <0.05 was considered significant.

RESULTS

Patient characteristics

Patients undergoing bariatric surgery were retrospectively grouped into CTRL (*n* = 16), NAFL (*n* = 10), and NASH (*n* = 32), as determined by histological examinations of their liver biopsies. All subjects were morbidly obese and most subjects complied with the definition of metabolic syndrome [i.e., large waist circumference (>89 cm for women and >102 cm for men, hyperglycemia (fasted glucose >5.6 mmol/l), hypertriglyceridaemia (>1.7 mmol/l), and reduced HDL cholesterol (<1.3 mmol/l in women and <1.04 mmol/l in men)]. Homeostatic model assessment of insulin resistance (HOMA-IR) (5.50 ± 0.51 vs. 3.06 ± 0.34) and blood glucose levels (6.9 ± 0.4 vs. 5.7 ± 0.3) were increased in NASH compared with CTRL, indicating a more insulin-resistant state. As expected, aspartate aminotransferase levels were higher in NASH compared with CTRL. When comparing NAFL to NASH, only glucose levels were significantly higher in individuals with NASH (Table 1).

Differences in hepatic lipid classes and species between CTRL, NAFL, and NASH

To investigate the hepatic lipidome in individuals with NAFL and NASH, the abundance of each lipid class was expressed relative to the CTRL group, with CTRL values set at 100%. Levels of TG, DG, acylcarnitine, dihydroceramide, dihexosylceramide, cholesterol, cholesteryl ester (CE), cardiolipin, and ubiquinone were significantly increased in NAFL and/or NASH groups compared with CTRL. Only acylcarnitine and dihexosylceramide were significantly higher in the NASH group compared with the NAFL group (Fig. 1, supplemental Table S2).

FA composition of TG and DG

Storage of excessive energy as TG is a feature and a key diagnostic criterion of NAFLD. Many of the TG and DG species were higher in the NAFL and NASH groups compared with the CTRL group. In the NASH group, nearly all TG, but not DG, species were significantly higher compared with the NAFL group (supplemental Table S3). To better understand changes in the FA composition of TGs

TABLE 1. Subject characteristics

Characteristics	Group		
	CTRL	NAFL	NASH
Number	16	10	32
Sex (% female)	81.3	90.0	65.6
Age (years)	42.3 \pm 2.5	41.6 \pm 3.9	45.5 \pm 1.8
BMI (kg/m ²)	41.0 \pm 1.6	45.5 \pm 2.4	48.39 \pm 1.9
Type II diabetes (%)	6.3	20.0	34.4
Glucose (mmol/l)	5.7 \pm 0.3	5.6 \pm 0.3	6.9 \pm 0.4 ^{a,b}
Insulin (mU/l)	12.3 \pm 1.3	20.0 \pm 3.5	18.8 \pm 1.9
HOMA-IR	3.06 \pm 0.34	4.96 \pm 0.76	5.50 \pm 0.51 ^a
HbA1c (%)	6.1 \pm 0.2	6.5 \pm 0.4	6.9 \pm 0.2
Total cholesterol (mmol/l)	4.74 \pm 0.22	5.20 \pm 0.31	4.97 \pm 0.19
HDL cholesterol (mmol/l)	1.13 \pm 0.09	0.95 \pm 0.08	1.02 \pm 0.08
LDL cholesterol (mmol/l)	2.76 \pm 0.21	3.30 \pm 0.36	2.99 \pm 0.17
TG (mmol/l)	1.87 \pm 0.24	1.98 \pm 0.32	2.22 \pm 0.21
Free FA (mmol/l)	0.51 \pm 0.06	0.59 \pm 0.12	0.92 \pm 0.19
ALT (U/l)	19.9 \pm 1.2	25.3 \pm 2.9	28.6 \pm 2.5
AST (U/l)	15.3 \pm 1.9	17.9 \pm 2.5	28.2 \pm 2.2 ^c
CRP (mg/l)	9.4 \pm 2.1	16.3 \pm 5.7	9.6 \pm 1.0

Baseline characteristics of CTRL, NAFL, and NASH groups are shown as percent (for categorical data) and mean \pm SEM (for nominal data). Data were analyzed using the chi-square test (categorical) or Mann-Whitney U test (nominal). HbA1c, hemoglobin A1c; AST, aspartate aminotransferase; ALT, alanine aminotransferase; CRP, C-reactive protein.

^a*P* < 0.05 versus CTRL.

^b*P* < 0.05 versus NAFL.

^c*P* < 0.01 versus CTRL.

and DGs between groups, FA composition was calculated as a percentage of total FAs of each lipid class (Fig. 2). Individuals with NASH had significantly more saturated FAs (SFAs) (i.e., 14:0 FA, 17:0 FA, and 18:0 FA) in their TGs compared with the CTRL group (Fig. 2A), whereas the most abundant SFA (16:0) did not change. The percentage of polyunsaturated arachidonic acid (20:4 FA) in TG was progressively lower in accordance with NAFLD severity. Interestingly, the percentage of docosahexaenoic acid (22:6 FA), which is another PUFA in TG, did not differ significantly between the groups (Fig. 2B). Although total levels of DG increased to a similar extent as TG with NAFL and NASH, there were disparities between the two lipid classes in terms of FA composition. Individuals with NAFL and NASH had higher levels of MUFAs in their DGs (16:1 FA and 18:1 FA). In contrast, percentages of SFA (18:0 FA), diunsaturated (DUFA, 18:2 FA), and long-chain PUFAs (20:4, 22:5, and 22:6) declined in the DG pool of the NAFL and NASH groups (Table 2, Fig. 2C, D).

FA composition of CEs

Like TGs and DGs, certain CEs comprised lipid species that were more abundant in the NAFL and NASH groups compared with the CTRL group (Fig. 1; supplemental Tables S2, S3). Among the most abundant FAs in CEs, 16:1 FA and 18:2 FA were increased in subjects with NASH compared with CTRL, while levels of 16:0 FA and 18:1 FA were decreased. The 16:0 FA was also significantly lower in NAFL individuals compared with CTRL (Fig. 3A). With respect to the less abundant FAs, 16:2 FA, 17:1 FA, 18:3 FA, and 22:6 FA were increased in the NASH group as compared with the CTRL group, while 20:1 FA, 20:2 FA, and 22:4 FA were decreased. The 16:2 FA was also significantly higher in the

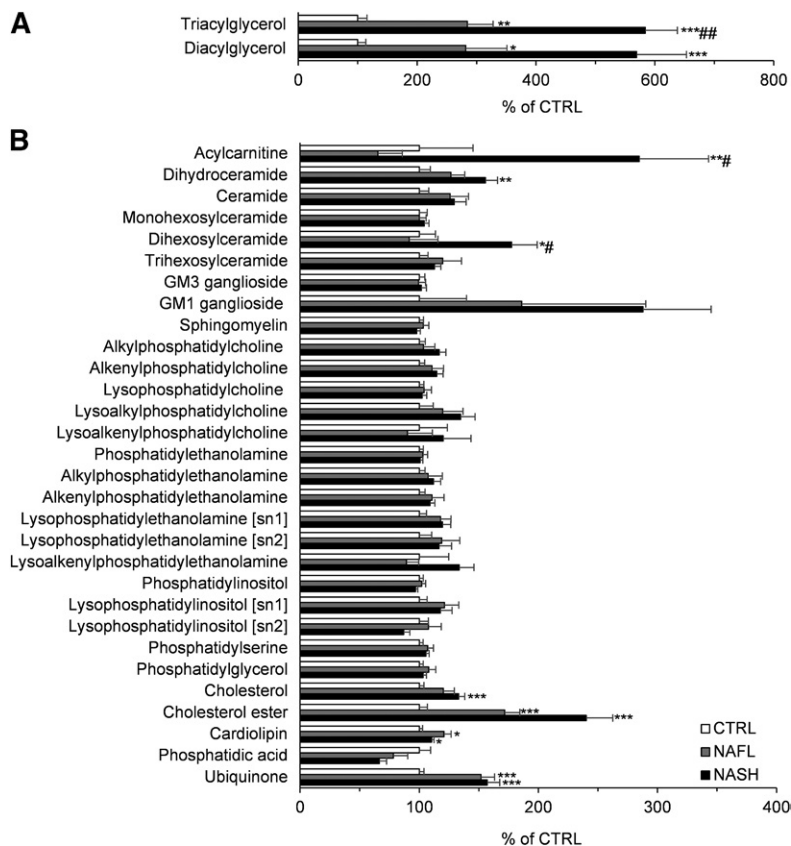


Fig. 1. Hepatic lipid abundance of the lipid classes/subclasses within the CTRL, NAFL, and NASH groups. Hepatic lipid abundance of the measured lipid classes and subclasses of NAFL (gray bars) and NASH (black bars) groups were compared with the CTRL (white bars) group and the result is presented as relative percent to CTRL. In panel A, the abundance of TG and DG are shown, and the rest of the lipid classes are shown in panel B. All values are expressed as mean \pm SEM. Data were analyzed with the Kruskal-Wallis test and corrected for multiple comparisons with the Benjamini-Hochberg approach. The Mann-Whitney U test corrected with the Dunn-Sidak approach was used for the post hoc analysis (n = 16 for CTRL; n = 10 for NAFL; n = 32 for NASH). * $P < 0.05$, ** $P < 0.01$, *** $P < 0.001$ versus CTRL; # $P < 0.05$, ## $P < 0.01$ versus NAFL.

NAFL group compared with CTRL and 20:2 FA was significantly lower in NASH compared with NAFL (Fig. 3B, C).

Phospholipids and sphingolipids

In contrast to TGs, DGs, and CEs, there were only a few differences among the phospholipid and sphingolipid species between groups (supplemental Tables S2, S3). Notably, several phospholipid species comprising docosa-hexaenoic acid (22:6 FA) were significantly lower when comparing individuals with NAFL and NASH, including

PC(P-16:0/22:6) (a) (NASH vs. NAFL), LPC 22:6[sn2] (NASH vs. CTRL), and PE (18:1_22:6) (a) (NASH vs. CTRL and NASH vs. NAFL). Furthermore, PC(40:7) and PC(40:8), which both contained 22:6 FA, were also lower in individuals with NASH compared with CTRL (Fig. 4A, supplemental Table S3). Although significant inter-group differences were not observed in any of the individual odd-chain PC species, logistic regression analysis indicated that total odd-chain PC was negatively associated with NAFLD. The odds ratio of total odd-chain PC, NASH versus CTRL, was 0.40 and reached statistical significance (Fig. 4A, B).

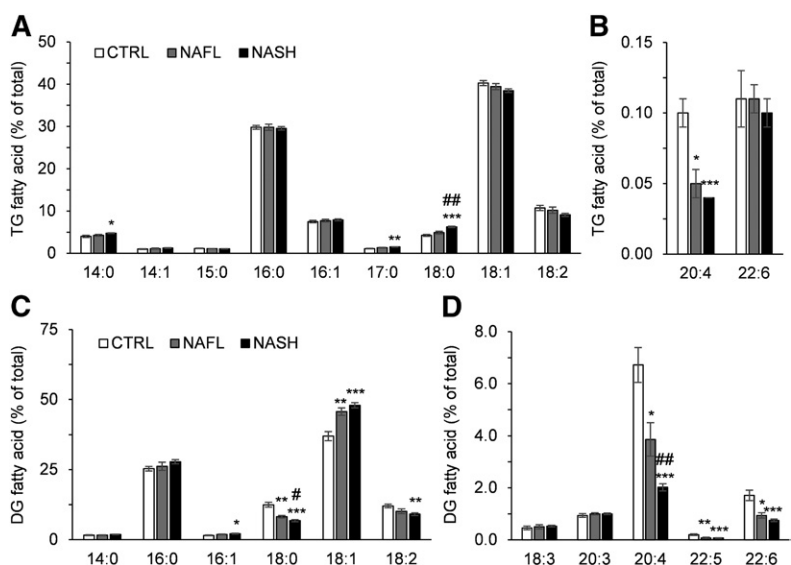


Fig. 2. FA composition of hepatic TG and DG in the CTRL, NAFL, and NASH groups. FAs comprising hepatic TG (A, B) and DG (C, D) are shown as the percent of total FA of the respective lipid classes in the CTRL (white bars), NAFL (gray bars), and NASH (black bars) groups. The FAs with high and low abundance in TG are presented in A and B, while the FAs with high and low abundance in DG are presented in C and D. All values are expressed as mean \pm SEM. Data were analyzed with the Kruskal-Wallis test and corrected for multiple comparisons with the Benjamini-Hochberg approach. The Mann-Whitney U test corrected with the Dunn-Sidak approach was used for the post hoc analysis (n = 16 for CTRL; n = 10 for NAFL; n = 32 for NASH). * $P < 0.05$, ** $P < 0.01$, *** $P < 0.001$ versus CTRL; # $P < 0.05$, ## $P < 0.01$ versus NAFL.

TABLE 2. Comparison of the FA saturation levels within the selected lipid classes between CTRL, NAFL, and NASH groups

	CTRL	NAFL	NASH
TG			
SFA	40.3 ± 0.66	41.4 ± 1.11	43.1 ± 0.50 ^a
MUFA	48.8 ± 0.57	48.3 ± 0.48	47.7 ± 0.42
DUFA	10.7 ± 0.62	10.2 ± 0.74	9.1 ± 0.37
PUFA	0.20 ± 0.02	0.16 ± 0.02	0.14 ± 0.01 ^a
DG			
SFA	39.4 ± 0.89	36.0 ± 1.47 ^b	36.5 ± 0.92
MUFA	38.5 ± 1.70	47.5 ± 1.26 ^a	50.1 ± 1.00 ^c
DUFA	12.0 ± 0.64	10.1 ± 0.86	9.10 ± 0.48 ^a
PUFA	10.0 ± 0.84	6.38 ± 0.66 ^b	4.36 ± 0.17 ^{c,d}
CE			
SFA	35.2 ± 0.69	32.8 ± 0.83	29.7 ± 0.60 ^{c,d}
MUFA	25.1 ± 0.91	22.7 ± 0.92	21.8 ± 0.80 ^b
DUFA	32.3 ± 1.08	35.9 ± 1.06	38.9 ± 1.11 ^a
PUFA	7.32 ± 0.49	8.61 ± 0.56	9.59 ± 0.36 ^a
Cardiolipin			
SFA	0.26 ± 0.05	0.38 ± 0.16	0.41 ± 0.08
MUFA	11.5 ± 0.44	12.8 ± 1.55	12.8 ± 0.36 ^b
DUFA	87.4 ± 0.47	86.0 ± 1.70	86.0 ± 0.38 ^b
PUFA	0.83 ± 0.08	0.76 ± 0.07	0.81 ± 0.06
Acylcarnitine			
SFA	62.7 ± 3.65	52.3 ± 4.69	57.9 ± 2.63
MUFA	25.0 ± 3.68	32.0 ± 3.97	36.0 ± 2.45 ^b
DUFA	12.3 ± 2.58	15.7 ± 4.85	6.19 ± 0.88
PUFA	—	—	—

Data in each lipid class are shown as mean ± SEM and were analyzed with the Kruskal-Wallis test and corrected for multiple comparisons with the Benjamini-Hochberg approach. The Mann-Whitney U test corrected with the Dunn-Sidak approach was the post hoc analysis (n = 16 for CTRL; n = 10 for NAFL; n = 32 for NASH).

^aP < 0.01 versus CTRL.

^bP < 0.05 versus CTRL.

^cP < 0.001 versus CTRL.

^dP < 0.05 versus NAFL.

In the sphingolipids class, only dihydroceramide and dihexosylceramide were significantly different between the CTRL and NAFLD groups. Interestingly, although both classes of sphingolipids were higher in individuals with NASH compared with CTRL, levels of dihydroceramide accumulated progressively with the disease severity (significant difference between NASH vs. CTRL), while levels of

dihexosylceramide were only increased in the NASH group (significant NASH vs. CTRL and NASH vs. NAFL) (Fig. 1, supplemental Table S2). In line with its respective lipid class, the dihydroceramide species, Cer(d18:0/18:0), was increased in the NAFL and NASH group compared with CTRL, while the dihexosylceramide species, Hex2Cer(d18:1/18:0) and Hex2Cer(d18:1/24:1), were only increased in the NASH group. The only SM species that differed between the groups was SM(38:1), which was lower in the NASH group compared with CTRL (supplemental Table S3).

Mitochondrial lipids and their FA composition in NAFLD

Mitochondrial dysfunction has been suggested to play a pivotal role in the pathogenesis of NAFLD (13, 14). Cardiolipin, acylcarnitine, and ubiquinone are lipid classes that have been linked to mitochondrial function (15, 16). Unlike other phospholipid classes, cardiolipin levels were significantly higher in the NAFL and NASH groups, as compared with the CTRL group (Fig. 1). When the FA composition of cardiolipin was analyzed, the percentage of 18:2 FA, the most abundant FA in the cardiolipin pool, was lower in NASH (not significant under Kruskal-Wallis test; Dunn-Sidak corrected Mann-Whitney U test P value = 0.039). The percentage of MUFAs was increased in NASH, while the percentage of diunsaturated FAs (DUFAs) was decreased (supplemental Table S4).

Nearly all acylcarnitine FAs were increased in individuals with NASH (supplemental Table S3). However, there were no differences in acylcarnitine FA composition between groups when expressed as a percentage of the total (supplemental Table S4). Some FAs showed a trend toward significance. Specifically, acylcarnitine 18:1 was increased in NASH compared with CTRL (not significant under Kruskal-Wallis test; Dunn-Sidak corrected Mann-Whitney U test P value = 0.015, NASH vs. CTRL), while acylcarnitine 18:2 was decreased in NASH versus CTRL (not significant under Kruskal-Wallis test; Dunn-Sidak

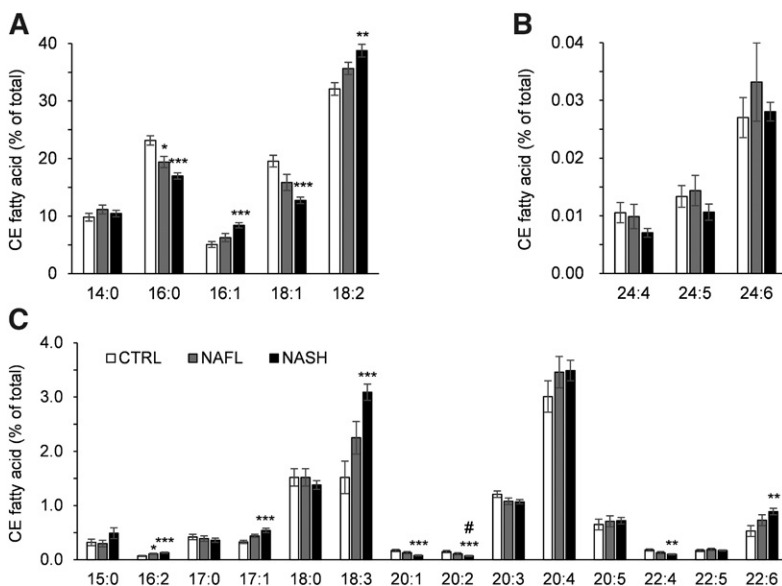


Fig. 3. FA composition of hepatic CE in the CTRL, NAFL, and NASH groups. FAs comprising hepatic CE are shown as the percent of total FA of the lipid class in the CTRL (white bars), NAFL (gray bars), and NASH (black bar) groups. Panels A, B, and C present the FAs with high, low, and medium abundance, respectively. All values are expressed as mean ± SEM. Data were analyzed with the Kruskal-Wallis test and corrected for multiple comparisons with the Benjamini-Hochberg approach. The Mann-Whitney U test corrected with the Dunn-Sidak approach was used for the post hoc analysis (n = 16 for CTRL; n = 10 for NAFL; n = 32 for NASH). *P < 0.05, **P < 0.01, ***P < 0.001 versus CTRL; #P < 0.05.

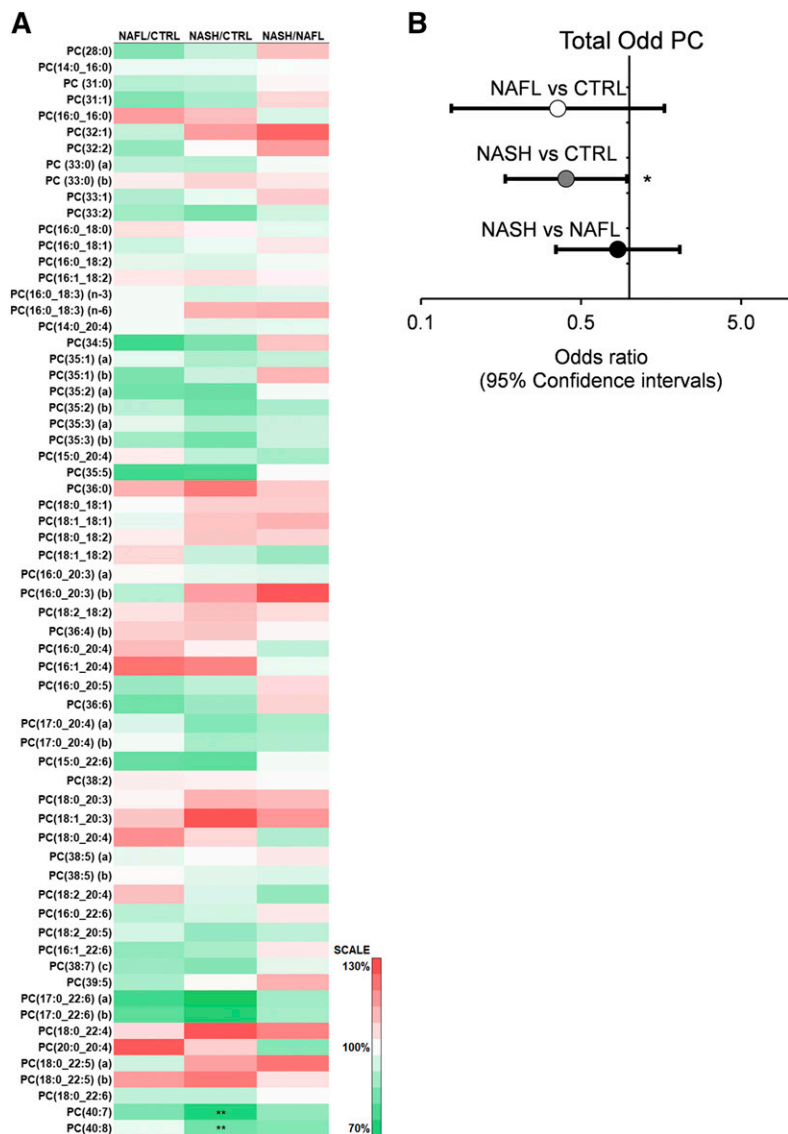


Fig. 4. Hepatic PC composition in the CTRL, NAFL, and NASH groups and the relationship of odd-chain PC to NAFLD. **A:** Heat map presentation of the fold differences in the PC species between the CTRL, NAFL, and NASH groups. **B:** The associations of total odd-chain PC to NAFLD, using logistic regression. Total odd-chain species were summed and log transformed before normalization to the interquartile ranges. The logistic regression was subsequently performed on NAFL versus CTRL (white), NASH versus CTRL (gray), and NASH versus NAFL (black). The data are shown as odds ratios and the error bars as the 95% confidence intervals. * $P < 0.05$; ** $P < 0.01$.

corrected Mann-Whitney U test P value = 0.082, NASH vs. CTRL) (supplemental Table S4). Levels of ubiquinone were increased with NAFL and NASH, compared with CTRL (Fig. 1).

NAFLD plasma lipidomics and its relationship to the hepatic lipidome

Several earlier studies examined the potential of predicting NAFLD by measuring plasma lipids (17, 18). However, none of the lipid biomarkers have been widely recognized as strong or reliable predictors to assess NAFLD in clinical settings. To investigate the possibility and accuracy of detecting NAFLD by assessing plasma lipids, we performed plasma lipid profiling using plasma samples from the CTRL, NAFL, and NASH subjects. The results were analyzed using logistic regression. Interestingly, acylcarnitines were the only plasma lipids that were significantly different between groups; more specifically, it was shown that acylcarnitines were increased in NASH versus CTRL subjects (Table 3, supplemental Tables S5, S6).

To determine how well plasma and hepatic lipidomes correlated, we performed Pearson correlations between the two datasets. While many plasma and hepatic lipid species correlated significantly, most of the highly correlated lipid species belonged to phospholipid classes (PC, alkylphosphatidylcholine, alkenylphosphatidylcholine, lysophosphatidylcholine, phosphatidylethanolamine, and phosphatidylinositol) and SM. Total acylcarnitine showed a high and positive correlation between the plasma and hepatic lipidomes (supplemental Tables S7, S8). Weaker, but significant, positive correlations were also found for dihydroceramides, monohexosylceramides, SMs, alkylphosphatidylcholines, phosphatidylserines, and TGs.

DISCUSSION

The hepatic and plasma lipidome changes extensively with the development of obesity and NAFLD, as demonstrated by earlier lipidomic studies (17–21). With a refined lipidomic platform, our study not only covered the most

TABLE 3. Plasma lipid species as potential predictors of NAFLD

	NAFL versus CTRL	NASH versus CTRL	NASH versus NAFL
OR >1	SM(41:1)	Acylcarnitine 12:0	Hex3Cer(d18:1/22:0)
	SM(42:1)	Acylcarnitine 14:1	SM(36:2) (a)
	Ubiquinone	Acylcarnitine 14:2	SM(38:1)
		Acylcarnitine 16:1	SM(41:1)
		PE(P-16:0/22:4)	SM(42:2) (b)
OR <1		CE(16:1)	PC(20:0_20:4)
		CE(17:1)	
		PC(35:2) (a)	PC(18:0_22:5) (a)
		PC(17:0_22:6) (a)	PI(40:5) (a)
		PC(40:7)	
		PC(40:8)	
		LPC 17:0[sn2]	
		PE(O-40:6)	
		LPE 16:0[sn2]	
		PI(40:5) (a)	

Data of CTRL, NAFL, and NASH groups were analyzed pairwise with logistic regression. Only lipid species with significant ($P < 0.05$) uncorrected P s are listed here. The (a) and (b) behind the lipid names of some species indicate that the lipid is one of the structural isomers separated by LC, but with an undetermined full chemical structure. Lipid species are categorized by the values of their odds ratios (OR).

common and abundant lipids, but also several low abundance and less studied lipid classes and species. Importantly, several classes/subclasses of lipids that differed significantly between the CTRL, NAFL, and NASH groups are related to mitochondrial dysfunction, a process that has been suggested to play an important role in the development of NAFLD. This study describes how hepatic and plasma lipid profiles are altered with NAFLD and highlights the possible implications of these changes on mitochondrial function and the progression of NAFLD.

In the current study, we found increased hepatic levels of TG, DG, CE, and free cholesterol in individuals with NAFLD, which is in congruence with earlier studies (19, 20). Also, the fatty acyl composition of these lipid classes was largely similar to earlier reports; there was a progressive decrease in percent PUFA in TGs and DGs, an increase in percent PUFA within CE, and an accumulation of free cholesterol in the NAFL and/or NASH groups. Furthermore, several PUFA-containing phospholipid species, especially those with docosahexanoic acid (22:6, n-3), decreased significantly in the NAFLD groups, which is again in line with studies reporting an increased n-6/n-3 ratio in NAFLD livers (19, 20).

Several recent studies suggest that mitochondrial dysfunction plays a key role in the development of advanced NAFLD. Hepatocytes are rich in mitochondria (~500–4,000 mitochondria per hepatocyte) (22), and mitochondrial abnormalities associated with NAFLD include abnormal morphological changes, leaking mitochondria, and oxidative stress (14, 23). In an elegant study by Koliaki et al. (14), it was recently shown that individuals with NAFL had ~5-fold higher hepatic mitochondrial respiration. Interestingly, this compensatory adaptation was abolished in BMI-matched individuals with NASH. The authors proposed that increased lipid availability in the liver of individuals with NAFL stimulates hepatic mitochondrial capacity and thereby serves to protect against NAFLD progression. However, increased respiration may not be bioenergetically

efficient due to leaking mitochondria and may promote excessive hepatic oxidative stress, challenging hepatocellular antioxidant defense mechanisms. Once these mechanisms fail, mitochondrial functionality decreases, resulting in the development of NASH (14).

Cardiolipin, ubiquinone, and acylcarnitine play an important role in mitochondrial function. Cardiolipin is a phospholipid that is required for optimal mitochondrial function (15). It is located in the inner mitochondrial membrane, where it interacts with and stabilizes mitochondrial enzymes and plays a role in maintaining inner membrane fluidity and osmotic stability (24). Cardiolipin is also important for mitochondrial biogenesis and the assembly of respiratory enzyme supercomplexes (25). Ubiquinone, also known as coenzyme Q10, is highly abundant in mitochondria (26). It is involved in the regulation of mitochondrial functions, such as membrane transition pore permeability and the activation of uncoupling proteins, and it acts as an anti-inflammatory agent and a lipophilic antioxidant protecting lipids, protein, and DNA from oxidation (16). Acylcarnitine is an intermediate, which is transported through the mitochondrial inner membrane and subsequently releases its attached fatty acyl group for β -oxidation (27).

Our study shows that hepatic cardiolipin and ubiquinone accumulated in NAFL, but did not increase further with NASH. Ferreira et al. (28) also observed increased levels of hepatic cardiolipin and ubiquinone in two diabetic rat models (Goto-Kakizaki and STZ-induced). Interestingly, both models of diabetes also presented a decreased susceptibility of liver mitochondria to the induction of mitochondrial permeability transition, a pore-opening reaction that is triggered by calcium and oxidative stress that leads to mitochondrial swelling and cell death. The authors suggested that the increase in cardiolipin and ubiquinone were compensatory processes aimed at preserving mitochondrial bioenergetic function (28). Similarly, we propose that the increased levels of cardiolipin and ubiquinone observed here are indicative of enhanced mitochondrial function, which may be invoked to maintain or boost mitochondrial function in response to the excessive energy substrate availability and/or hepatic insulin resistance. In support of this hypothesis, recent studies in rats with NAFLD found increased liver cardiolipin levels (29, 30), and these levels correlated positively to in vitro measures of mitochondrial membrane potential and respiration (30). Furthermore, increased mitochondrial respiration has previously been observed in patients with hepatic steatosis (14). Importantly though, excess cardiolipin has also been shown to have detrimental effects on mitochondria. Cardiolipin is highly susceptible to peroxidation due to its close association with respiratory chain proteins, which may result in induction of the apoptotic cascade that ultimately leads to programmed cell death (31–33). Indeed, cardiolipin peroxidation is associated with mitochondrial dysfunction in several pathophysiological conditions, including NAFLD (30–33). We also observed an increase in cardiolipin MUFA percent and a decrease in DUFA percent (mostly linoleic acid, C18:2). Similar alterations in cardiolipin

composition have previously been shown to compromise mitochondrial function by disrupting the highly symmetric FA distribution (i.e., identical FAs are often found in both *sn*-1 positions and in both *sn*-2 positions) and have also been linked to Barth syndrome, a childhood onset of dilated cardiomyopathy and neutropenia associated with mitochondrial respiratory chain dysfunction (15, 34, 35). It is also relevant that the fold increase of hepatic ubiquinone was higher than observed for cardiolipin (152% and 122% vs. respective controls). Because cardiolipin has been suggested to promote electron transport between complex I and ubiquinone, it is possible that the disproportionate changes in cardiolipin and ubiquinone create an unfavorable environment for optimal electron transport (36).

Levels of acylcarnitine were significantly increased in individuals with NASH, but not in individuals with NAFL, as compared with the CTRL group. The accumulation of acylcarnitine is suggested to be a sign of mitochondrial stress, mitochondrial dysfunction, and impaired FA oxidation (37–39). Our results corroborate that acylcarnitine accumulation reflects mitochondrial dysfunction and is a hallmark event of NASH. Our data also support the view of Koliaki et al. (14), that increased lipid availability in the liver stimulates hepatic mitochondrial capacity to protect against NAFLD progression. We suggest that levels of cardiolipin and ubiquinone are increased in individuals with NAFLD, in an attempt to boost mitochondrial respiration, but that mitochondrial function eventually fails, leading to increased levels of acylcarnitine and NASH (Fig. 5). We have, however, no measures of mitochondrial function in our study and, therefore, it was not possible to directly link lipid classes to mitochondrial function. Such possibilities will be the focus of future investigations.

We observed a negative association between hepatic odd-chain PC and NAFLD. Emerging evidence suggests that a noticeable portion of odd-chain FA can be derived from branched-chain amino acids (BCAAs; i.e., valine, leucine, and isoleucine) (40, 41). Because the majority of enzymes involved in BCAA catabolism reside in mitochondria (42), the odd-chain PC, although of low abundance, is a likely indicator of mitochondrial BCAA catabolic capacity. We

therefore propose that the impairment of BCAA catabolism due to hepatic mitochondrial dysfunction may be responsible for the negative association between odd-chain PC and NAFLD. In support of this interpretation, Lefort et al. (43) previously isolated mitochondria from the skeletal muscle of insulin-resistant individuals, and reported specific abundance differences in proteins involved in BCAA oxidation. Specifically, methylmalonate semialdehyde dehydrogenase and propionyl-CoA carboxylase, mitochondrial proteins that are required for valine and isoleucine metabolism before entry into the tricarboxylic acid cycle as succinyl-CoA, were decreased in mitochondria of obese individuals. The authors suggested that this might contribute to the accumulation of BCAA that is frequently associated with the pathogenesis of insulin resistance (43). Our viewpoint is further supported by metabolomic studies showing increased hepatic BCAA levels in individuals with NAFLD (39, 44, 45). Thus, our study provides new potential explanations regarding the low circulating odd-chain PC and high BCAAs observed in NAFLD and type 2 diabetes patients (46–48).

Although we did not see an increase in ceramide in NAFLD, our data do suggest activation of the de novo ceramide biosynthetic pathway, as indicated by progressive accumulation of dihydroceramides. This phenomenon is possibly a consequence of increased SFAs in NAFLD liver (49). A recent study also observed increased levels of dihydroceramide species in obese individuals with NASH compared with lean healthy control subjects, and reported a positive association between total hepatic dihydroceramide levels and hepatic oxidative stress and inflammation (50). At the cellular level, increased levels of dihydroceramides can regulate autophagy, reactive oxygen species production, cell proliferation, and apoptosis (51, 52), which can cause fibrosis (52). Thus, there is accumulating evidence that increased dihydroceramide may contribute to the progression of NAFLD and related metabolic disorders.

We also observed increased levels of dihexosylceramide in individuals with NASH, but not with NAFL. We previously reported a positive association between circulating dihexosylceramides and alcoholic liver cirrhosis (6), and

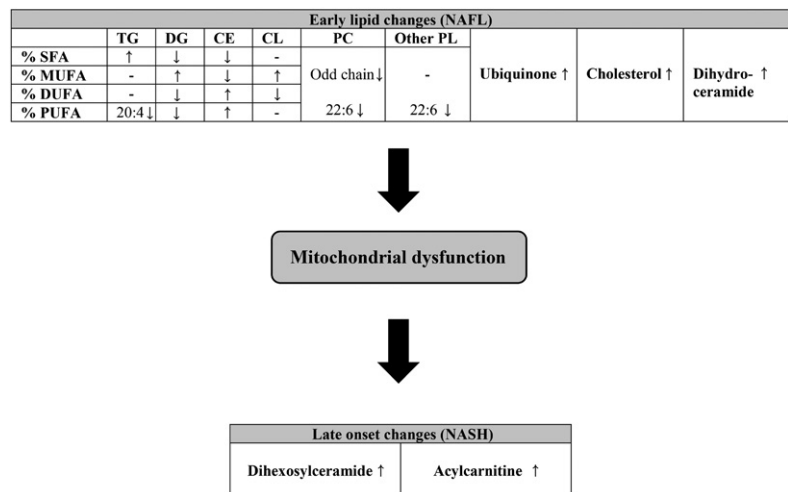



Fig. 5. Schematic presentation of the proposed changes in the hepatic lipidome during the progression of NAFL to NASH: a central role of mitochondrial stress and dysfunction. At the early stage of NAFLD, there is accumulation of hepatic levels of TG, DG, CE, and cardiolipin (CL). This is accompanied by changes in the FA composition. Total ubiquinone, cholesterol, and dihydroceramide also accumulate at this stage. The increase in cardiolipin and ubiquinone may serve as a compensatory mechanism to boost mitochondrial respiration. The transition from NAFL to NASH is possibly driven by mitochondrial dysfunction, resulting in increased levels of dihexosylceramide and acylcarnitine. PL, phospholipid.

increased levels of hepatic dihexosylceramide have been detected in human hepatocellular carcinoma tissues compared with the surrounding noncancerous hepatic tissues (53). Animal studies showed that pharmacological inhibitions of glucosylceramide synthase could improve insulin sensitivity and steatosis (54–56). These observations provide a strong rationale for further investigation of dihexosylceramides in the transition from NAFLD to NASH, and possibly hepatocellular carcinoma.

In conclusion, our lipidomic study provides an overview of the hepatic lipidome and outlines the putative links between mitochondrial and cellular lipids and mitochondrial dysfunction. We provide clinically relevant information describing the lipidomic changes during the transition from NAFL to NASH. This is important for understanding the pathogenesis of this disease. We propose that cardiolipin and ubiquinone levels increase in NAFL to enhance mitochondrial function, perhaps as a compensatory mechanism to reduce steatosis; whereas, the increased levels of acylcarnitine in NASH are reflective of mitochondrial dysfunction with the progression of disease. The negative association between odd-chain PC and NAFLD is another novel finding, which possibly reflects impaired mitochondrial BCAA catabolism. The finding of increased dihydroceramides and dihexosylceramides with NAFLD provides an intriguing addition to our understanding of sphingolipid (e.g., ceramide) metabolism in NAFLD. Our findings provide the clinical rationale to pursue studies aimed at understanding the mechanistic relevance of these lipid types in NAFLD pathogenesis. 

The authors wish to thank Natalie Mellett and Jaquelyn Weir for technical support with the lipidomic analysis.

REFERENCES

- Silverman, J. F., K. F. O'Brien, S. Long, N. Leggett, P. G. Khazanie, W. J. Pories, H. T. Norris, and J. F. Caro. 1990. Liver pathology in morbidly obese patients with and without diabetes. *Am. J. Gastroenterol.* **85**: 1349–1355.
- Schwenger, K. J. P., S. E. Fischer, T. D. Jackson, A. Okrainec, and J. P. Allard. 2018. Non-alcoholic fatty liver disease in morbidly obese individuals undergoing bariatric surgery: prevalence and effect of the pre-bariatric very low calorie diet. *Obes. Surg.* **28**: 1109–1116.
- Fotbolcu, H., and E. Zorlu. 2016. Nonalcoholic fatty liver disease as a multi-systemic disease. *World J. Gastroenterol.* **22**: 4079–4090.
- Meex, R. C. R., and M. J. Watt. 2017. Hepatokines: linking nonalcoholic fatty liver disease and insulin resistance. *Nat. Rev. Endocrinol.* **13**: 509–520.
- Sa, R., W. Zhang, J. Ge, X. Wei, Y. Zhou, D. R. Landzberg, Z. Wang, X. Han, L. Chen, and H. Yin. 2016. Discovering a critical transition state from nonalcoholic hepatosteatosis to nonalcoholic steatohepatitis by lipidomics and dynamical network biomarkers. *J. Mol. Cell Biol.* **8**: 195–206.
- Meikle, P. J., P. A. Mundra, G. Wong, K. Rahman, K. Huynh, C. K. Barlow, A. M. Duly, P. S. Haber, J. B. Whitfield, and D. Seth. 2015. Circulating lipids are associated with alcoholic liver cirrhosis and represent potential biomarkers for risk assessment. *PLoS One.* **10**: e0130346.
- Brunt, E. M., C. G. Janney, A. M. Di Bisceglie, B. A. Neuschwander-Tetri, and B. R. Bacon. 1999. Nonalcoholic steatohepatitis: a proposal for grading and staging the histological lesions. *Am. J. Gastroenterol.* **94**: 2467–2474.
- Kleiner, D. E., E. M. Brunt, M. Van Natta, C. Behling, M. J. Contos, O. W. Cummings, L. D. Ferrell, Y. C. Liu, M. S. Torbenson, A. Unalp-Arida, et al.; Nonalcoholic Steatohepatitis Clinical Research Network. 2005. Design and validation of a histological scoring system for nonalcoholic fatty liver disease. *Hepatology.* **41**: 1313–1321.
- Meikle, P. J., G. Wong, D. Tzorotes, C. K. Barlow, J. M. Weir, M. J. Christopher, G. L. MacIntosh, B. Goudey, L. Stern, and A. Kowalczyk. 2011. Plasma lipidomic analysis of stable and unstable coronary artery disease. *Arterioscler. Thromb. Vasc. Biol.* **31**: 2723–2732.
- Weir, J. M., G. Wong, C. K. Barlow, M. A. Greeve, A. Kowalczyk, L. Almasy, A. G. Comuzzie, M. C. Mahaney, J. B. Jowett, and J. Shaw. 2013. Plasma lipid profiling in a large population-based cohort. *J. Lipid Res.* **54**: 2898–2908.
- Hsu, F. F., and J. Turk. 2003. Electrospray ionization/tandem quadrupole mass spectrometric studies on phosphatidylcholines: the fragmentation processes. *J. Am. Soc. Mass Spectrom.* **14**: 352–363.
- Hsu, F. F., J. Turk, A. K. Thukkani, M. C. Messner, K. R. Wildsmith, and D. A. Ford. 2003. Characterization of alkylacyl, alk-1-enylacyl and lyso subclasses of glycerophosphocholine by tandem quadrupole mass spectrometry with electrospray ionization. *J. Mass Spectrom.* **38**: 752–763.
- Begrache, K., A. Igoudjil, D. Pessayre, and B. Fromenty. 2006. Mitochondrial dysfunction in NASH: causes, consequences and possible means to prevent it. *Mitochondrion.* **6**: 1–28.
- Koliaki, C., J. Szendroedi, K. Kaul, T. Jelenik, P. Nowotny, F. Jankowiak, C. Herder, M. Carstensen, M. Krausch, W. T. Knoefel, et al. 2015. Adaptation of hepatic mitochondrial function in humans with non-alcoholic fatty liver is lost in steatohepatitis. *Cell Metab.* **21**: 739–746.
- Chicco, A. J., and G. C. Sparagna. 2007. Role of cardiolipin alterations in mitochondrial dysfunction and disease. *Am. J. Physiol. Cell Physiol.* **292**: C33–C44.
- Botham, K. M., M. Napolitano, and E. Bravo. 2015. The emerging role of disturbed CoQ metabolism in nonalcoholic fatty liver disease development and progression. *Nutrients.* **7**: 9834–9846.
- Anjani, K., M. Lhomme, N. Sokolovska, C. Poitou, J. Aron-Wisniewsky, J. L. Bouillot, P. Lesnik, P. Bedossa, A. Kontush, K. Clement, et al. 2015. Circulating phospholipid profiling identifies portal contribution to NASH signature in obesity. *J. Hepatol.* **62**: 905–912.
- Gorden, D. L., D. S. Myers, P. T. Ivanova, E. Fahy, M. R. Maurya, S. Gupta, J. Min, N. J. Spann, J. G. McDonald, S. L. Kelly, et al. 2015. Biomarkers of NAFLD progression: a lipidomics approach to an epidemic. *J. Lipid Res.* **56**: 722–736.
- Araya, J., R. Rodrigo, L. A. Videla, L. Thielemann, M. Orellana, P. Pettinelli, and J. Poniachik. 2004. Increase in long-chain polyunsaturated fatty acid n-6/n-3 ratio in relation to hepatic steatosis in patients with non-alcoholic fatty liver disease. *Clin. Sci. (Lond.)* **106**: 635–643.
- Puri, P., R. A. Baillie, M. M. Wiest, F. Mirshahi, J. Choudhury, O. Cheung, C. Sargeant, M. J. Contos, and A. J. Sanyal. 2007. A lipidomic analysis of nonalcoholic fatty liver disease. *Hepatology.* **46**: 1081–1090.
- Puri, P., M. M. Wiest, O. Cheung, F. Mirshahi, C. Sargeant, H. K. Min, M. J. Contos, R. K. Sterling, M. Fuchs, H. Zhou, et al. 2009. The plasma lipidomic signature of nonalcoholic steatohepatitis. *Hepatology.* **50**: 1827–1838.
- Degli Esposti, D., J. Hamelin, N. Bosselut, R. Saffroy, M. Sebah, A. Pommier, C. Martel, and A. Lemoine. 2012. Mitochondrial roles and cytoprotection in chronic liver injury. *Biochem. Res. Int.* **2012**: 387626.
- Rolo, A. P., J. S. Teodoro, and C. M. Palmeira. 2012. Role of oxidative stress in the pathogenesis of nonalcoholic steatohepatitis. *Free Radic. Biol. Med.* **52**: 59–69.
- Schlame, M. 2008. Cardiolipin synthesis for the assembly of bacterial and mitochondrial membranes. *J. Lipid Res.* **49**: 1607–1620.
- Pfeiffer, K., V. Gohil, R. A. Stuart, C. Hunte, U. Brandt, M. L. Greenberg, and H. Schagger. 2003. Cardiolipin stabilizes respiratory chain supercomplexes. *J. Biol. Chem.* **278**: 52873–52880.
- Stefely, J. A., and D. J. Pagliarini. 2017. Biochemistry of mitochondrial coenzyme Q biosynthesis. *Trends Biochem. Sci.* **42**: 824–843.
- Schooneman, M. G., F. M. Vaz, S. M. Houten, and M. R. Soeters. 2013. Acylcarnitines: reflecting or inflicting insulin resistance? *Diabetes.* **62**: 1–8.
- Ferreira, F. M., R. Seica, P. J. Oliveira, P. M. Coxito, A. J. Moreno, C. M. Palmeira, and M. S. Santos. 2003. Diabetes induces metabolic adaptations in rat liver mitochondria: role of coenzyme Q and cardiolipin contents. *Biochim. Biophys. Acta.* **1639**: 113–120.

29. Aoun, M., G. Fouret, F. Michel, B. Bonafos, J. Ramos, J. P. Cristol, M. A. Carbonneau, C. Coudray, and C. Feillet-Coudray. 2012. Dietary fatty acids modulate liver mitochondrial cardiolipin content and its fatty acid composition in rats with nonalcoholic fatty liver disease. *J. Bioenerg. Biomembr.* **44**: 439–452.
30. Fouret, G., S. Gaillet, J. Lecomte, B. Bonafos, F. Djohan, B. Barea, E. Badia, C. Coudray, and C. Feillet-Coudray. 2018. 20-Week follow-up of hepatic steatosis installation and liver mitochondrial structure and activity and their interrelation in rats fed a high-fat-high-fructose diet. *Br. J. Nutr.* **119**: 368–380.
31. Petrosillo, G., F. M. Ruggiero, M. Pistolese, and G. Paradies. 2001. Reactive oxygen species generated from the mitochondrial electron transport chain induce cytochrome c dissociation from beef-heart submitochondrial particles via cardiolipin peroxidation. Possible role in the apoptosis. *FEBS Lett.* **509**: 435–438.
32. Paradies, G., V. Paradies, F. M. Ruggiero, and G. Petrosillo. 2014. Oxidative stress, cardiolipin and mitochondrial dysfunction in non-alcoholic fatty liver disease. *World J. Gastroenterol.* **20**: 14205–14218.
33. Paradies, G., G. Petrosillo, M. Pistolese, and F. M. Ruggiero. 2002. Reactive oxygen species affect mitochondrial electron transport complex I activity through oxidative cardiolipin damage. *Gene.* **286**: 135–141.
34. Houtkooper, R. H., M. Turkenburg, B. T. Poll-The, D. Karall, C. Perez-Cerda, A. Morrone, S. Malvagia, R. J. Wanders, W. Kulik, and F. M. Vaz. 2009. The enigmatic role of tafazzin in cardiolipin metabolism. *Biochim. Biophys. Acta.* **1788**: 2003–2014.
35. Schlame, M., M. Ren, Y. Xu, M. L. Greenberg, and I. Haller. 2005. Molecular symmetry in mitochondrial cardiolipins. *Chem. Phys. Lipids.* **138**: 38–49.
36. Vos, M., A. Geens, C. Bohm, L. Deaulmerie, J. Swerts, M. Rossi, and K. Craessaerts. 2017. Cardiolipin promotes electron transport between ubiquinone and complex I to rescue PINK1 deficiency 216: 695–708.
37. Pérez-Carreras, M., P. Del Hoyo, M. A. Martín, J. C. Rubio, A. Martín, G. Castellano, F. Colina, J. Arenas, and J. A. Solís-Herruzo. 2003. Defective hepatic mitochondrial respiratory chain in patients with nonalcoholic steatohepatitis. *Hepatology.* **38**: 999–1007.
38. Lake, A. D., P. Novak, P. Shipkova, N. Aranibar, D. G. Robertson, M. D. Reily, L. D. Lehman-McKeeman, R. R. Vaillancourt, and N. J. Cherrington. 2015. Branched chain amino acid metabolism profiles in progressive human nonalcoholic fatty liver disease. *Amino Acids.* **47**: 603–615.
39. Patterson, R. E., S. Kalavalapalli, C. M. Williams, M. Nautiyal, J. T. Mathew, J. Martinez, M. K. Reinhard, D. J. McDougall, J. R. Rocca, R. A. Yost, et al. 2016. Lipotoxicity in steatohepatitis occurs despite an increase in tricarboxylic acid cycle activity. *Am. J. Physiol. Endocrinol. Metab.* **310**: E484–E494.
40. Green, C. R., M. Wallace, A. S. Divakaruni, S. A. Phillips, A. N. Murphy, T. P. Ciaraldi, and C. M. Metallo. 2016. Branched-chain amino acid catabolism fuels adipocyte differentiation and lipogenesis. *Nat. Chem. Biol.* **12**: 15–21.
41. Crown, S. B., N. Marze, and M. R. Antoniewicz. 2015. Catabolism of branched chain amino acids contributes significantly to synthesis of odd-chain and even-chain fatty acids in 3T3-L1 adipocytes. *PLoS One.* **10**: e0145850.
42. Lynch, C. J., and S. H. Adams. 2014. Branched-chain amino acids in metabolic signalling and insulin resistance. *Nat. Rev. Endocrinol.* **10**: 723–736.
43. Lefort, N., B. Glancy, B. Bowen, W. T. Willis, Z. Bailowitz, E. A. De Filippis, C. Brophy, C. Meyer, K. Hojlund, Z. Yi, et al. 2010. Increased reactive oxygen species production and lower abundance of complex I subunits and carnitine palmitoyltransferase 1B protein despite normal mitochondrial respiration in insulin-resistant human skeletal muscle. *Diabetes.* **59**: 2444–2452.
44. Kaikkonen, J. E., P. Wurtz, E. Suomela, M. Lehtovirta, A. J. Kangas, A. Jula, V. Mikkila, J. S. Viikari, M. Juonala, T. Ronnema, et al. 2017. Metabolic profiling of fatty liver in young and middle-aged adults: cross-sectional and prospective analyses of the Young Finns Study. *Hepatology.* **65**: 491–500.
45. Goffredo, M., N. Santoro, D. Trico, C. Giannini, E. D'Adamo, H. Zhao, G. Peng, X. Yu, T. T. Lam, B. Pierpont, et al. 2017. A branched-chain amino acid-related metabolic signature characterizes obese adolescents with non-alcoholic fatty liver disease. *Nutrients.* **9**: E642.
46. Kulkarni, H., P. J. Meikle, M. Mamtani, J. M. Weir, C. K. Barlow, J. B. Jowett, C. Bellis, T. D. Dyer, M. P. Johnson, D. L. Rainwater, et al. 2013. Variability in associations of phosphatidylcholine molecular species with metabolic syndrome in Mexican-American families. *Lipids.* **48**: 497–503.
47. Forouhi, N. G., A. Koulman, S. J. Sharp, F. Imamura, J. Kroger, M. B. Schulze, F. L. Crowe, J. M. Huerta, M. Guevara, J. W. Beulens, et al. 2014. Differences in the prospective association between individual plasma phospholipid saturated fatty acids and incident type 2 diabetes: the EPIC-InterAct case-cohort study. *Lancet Diabetes Endocrinol.* **2**: 810–818.
48. Su, X., F. Magkos, D. Zhou, J. C. Eagon, E. Fabbrini, A. L. Okunade, and S. Klein. 2015. Adipose tissue monomethyl branched-chain fatty acids and insulin sensitivity: effects of obesity and weight loss. *Obesity (Silver Spring).* **23**: 329–334.
49. Pagadala, M., T. Kasumov, A. J. McCullough, N. N. Zein, and J. P. Kirwan. 2012. Role of ceramides in nonalcoholic fatty liver disease. *Trends Endocrinol. Metab.* **23**: 365–371.
50. Apostolopoulou, M., R. Gordillo, C. Koliaki, S. Gancheva, T. Jelenik, E. De Filippo, C. Herder, D. Markgraf, F. Jankowiak, I. Esposito, et al. 2018. Specific hepatic sphingolipids relate to insulin resistance, oxidative stress, and inflammation in nonalcoholic steatohepatitis. *Diabetes Care.* **41**: 1235–1243.
51. Rodriguez-Cuenca, S., N. Barbarroja, and A. Vidal-Puig. 2015. Dihydroceramide desaturase 1, the gatekeeper of ceramide induced lipotoxicity. *Biochim. Biophys. Acta.* **1851**: 40–50.
52. Lee, A. Y., J. W. Lee, J. E. Kim, H. J. Mock, S. Park, S. Kim, S. H. Hong, J. Y. Kim, E. J. Park, K. S. Kang, et al. 2017. Dihydroceramide is a key metabolite that regulates autophagy and promotes fibrosis in hepatic steatosis model. *Biochem. Biophys. Res. Commun.* **494**: 460–469.
53. Okada, Y., T. Arima, H. Hada, M. Fukushima, J. Watanabe, and H. Nagashima. 1985. Human hepatocellular carcinoma is associated with quantitative and qualitative changes in glycolipids. *Liver.* **5**: 226–235.
54. Zhao, H., M. Przybylska, I. H. Wu, J. Zhang, C. Siegel, S. Komarnitsky, N. S. Yew, and S. H. Cheng. 2007. Inhibiting glycosphingolipid synthesis improves glycemic control and insulin sensitivity in animal models of type 2 diabetes. *Diabetes.* **56**: 1210–1218.
55. Zhao, H., M. Przybylska, I. H. Wu, J. Zhang, P. Maniatis, J. Pacheco, P. Piepenhagen, D. Copeland, C. Arbeen, J. A. Shayman, et al. 2009. Inhibiting glycosphingolipid synthesis ameliorates hepatic steatosis in obese mice. *Hepatology.* **50**: 85–93.
56. Bijl, N., M. Sokolovic, C. Vrins, M. Langeveld, P. D. Moerland, R. Ottenhoff, C. P. van Roomen, N. Claessen, R. G. Boot, J. Aten, et al. 2009. Modulation of glycosphingolipid metabolism significantly improves hepatic insulin sensitivity and reverses hepatic steatosis in mice. *Hepatology.* **50**: 1431–1441.